Z-ring force and cell shape during division in rod-like bacteria

Ganhui Lan*, Charles W. Wolgemuth†, and Sean X. Sun*‡§

*Department of Mechanical Engineering and ‡Whitaker Institute of Biomedical Engineering, The Johns Hopkins University, Baltimore, MD 21218; and †Department of Cell Biology and Center for Cell Analysis and Modeling, University of Connecticut Health Center, Farmington, CT 06030-3505

Edited by Michael E. Fisher, University of Maryland, College Park, MD, and approved August 21, 2007 (received for review March 29, 2007)

The life cycle of bacterial cells consists of repeated elongation, septum formation, and division. Before septum formation, a division ring called the Z-ring, which is made of a filamentous tubulin analog, FtsZ, is seen at the mid cell. Together with several other proteins, FtsZ is essential for cell division. Visualization of strains with GFP-labeled FtsZ shows that the Z-ring contracts before septum formation and pinches the cell into two equal halves. Thus, the Z-ring has been postulated to act as a force generator, although the magnitude of the contraction force is unknown. In this article, we develop a mathematical model to describe the process of growth and Z-ring contraction in rod-like bacteria. The elasticity and growth of the cell wall is incorporated in the model to predict the contraction speed, the cell shape, and the contraction force. With reasonable parameters, the model shows that a small force from the Z-ring (8 pN in *Escherichia coli*) is sufficient to accomplish division.

bacterial cell division | FtsZ-ring | mathematical model | peptidoglycan synthesis

In rod-like bacteria, such as *Escherichia coli* and *Bacillus subtilis*, a conserved cell division gene is FtsZ, which forms a filamentous ring structure (Z-ring) at the mid cell before division (1, 2). The positioning of the Z-ring at the mid cell in *E. coli* is related to spatial–temporal oscillations in the MinCDE system (3–5). For the actual division step, the radius of the Z-ring is seen to decrease over several minutes, after which a septum is formed and the bacterium separates into two daughter cells (1, 6). It has been postulated that the Z-ring generates forces and "pinches" the cell into halves (7), although whether FtsZ generates force is debatable. In addition to the Fts family of proteins, other proteins are also essential for cell division. In particular, disabling peptidoglycan (PG) synthesis proteins or penicillin binding proteins (PBP) just before division stops cytokinesis (8, 9). A systematic study showed that some PBPs are localized near the Z-ring during division (10). Therefore, cell wall synthesis is important in cell division. The mechanics and the dynamics of the cell wall must be considered on an equal footing for quantifying bacterial cell division.

Growth and synthesis of the bacterial cell wall is a complex process. The wall is composed of saccharide strands interconnected by polypeptides (7, 11–13). Indeed, families of PBPs are found in bacteria, with some localized near the furrow during division and some uniformly distributed (10, 14, 15). Coordinated activity of PBPs synthesizes new PG strands, cross-linking them into the existing wall structure. In a proposed growth model, old strands are also depolymerized, thereby removing them from the wall structure (a process that we will generically call "turnover") (7, 11, 16), although models for *E. coli* growth without turnover also have been proposed (12, 13). Using radio-active labeling, turnover in the PG layer has been investigated (17–19). It was found that the cell wall turns over a significant fraction of its mass in one life cycle. The polar cap regions, however, turn over much more slowly during the growing phase of the bacterium (20). In *B. subtilis*, which lacks an outer membrane, removed old strands have been detected in the surrounding medium (17, 21). In *E. coli*, which has an outer membrane, old strands are probably recycled in the growth mechanism (18, 19). Even though the cell wall structure is complex, it can be viewed as an elastic mechanical structure. The mechanical properties of the PG cell wall have been investigated, and the Young's moduli for several bacteria have been estimated (22, 23). In Gram-positive bacteria, such as *B. subtilis*, the PG layer is relatively thick (≈40 nm) (24) and mechanically rigid. In Gram-negative bacteria, such as *E. coli*, the PG layer is thin (≈6 nm) (21), and the wall is significantly softer.

Motor proteins have not been discovered for prokaryotic cells, and the mechanism of Z-ring contraction is unknown. How are wall mechanics, wall growth, and Z-ring contraction combined to achieve cell division? This article develops a mathematical model of bacterial cell division that incorporates realistic cell wall mechanical properties. The model also considers the kinetics of cell wall growth and turnover and gives a mechanism and quantitative description of cell wall viscoelasticity. The model predicts that a small force from the Z-ring (as low as 8 pN in *E. coli*) is sufficient to accomplish division. The most critical factor in generating realistic cell shapes during division is the wall growth kinetics, which determine the contraction speed.

The Model

Description of the Model. Our model of bacterial cell division has four major components: First, the mechanics of the primary structural component, the cell wall, is defined. The static cell shape is determined by how the wall responds to applied force. Specifically, the FtsZ-ring applies a localized and radially inward force at the division site. Second, internal turgor pressure must be included. The cell is inflated throughout the cell cycle. Third, growth of the cell wall adds new material to the existing cell wall. The manner of cell wall change is determined by the growth mechanism. Finally, during division, some PBPs are localized at the division site, leading to faster growth and wall synthesis near the division site. The localization is related to forces exerted by the Z-ring, which facilitates the breakage of existing PG cross-linkers. These four components are described by a coupled set of equations specified in supporting information (SI) *Text*. The following paragraphs give a qualitative description of these components.

Mechanics of Bacterial Cell Wall. The bacterial cell wall is a relatively rigid material. Bacterial cells also maintain a constant

Author contributions: G.L., C.W.W., and S.X.S. designed research; G.L. and S.X.S. performed research; and C.W.W. and S.X.S. wrote the paper.

The authors declare no conflict of interest.

This article is a PNAS Direct Submission.

Abbreviations: PBP, penicillin binding protein; PG, peptidoglycan.

§To whom correspondence should be addressed. E-mail: ssun@jhu.edu.

This article contains supporting information online at www.pnas.org/cgi/content/full/0702925104/DC1.

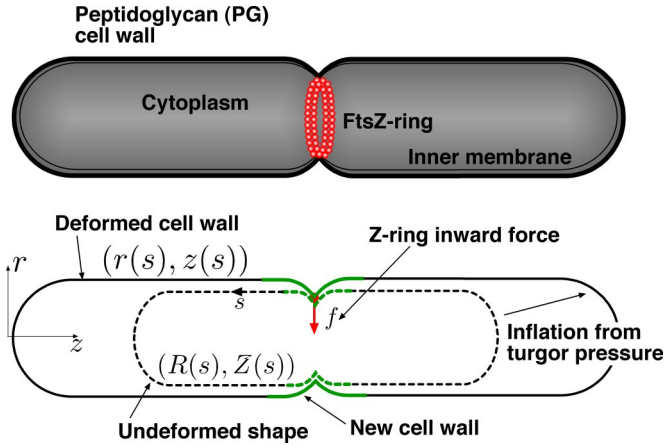

Fig. 1. A mechanical model of bacterial cell division. The FtsZ-ring is positioned at the mid cell and generates a contractile force, *f*, in the inward radial direction (red arrow). The observed PG cell wall is inflated from the undeformed cell shape by internal turgor pressure, much like a balloon. The undeformed cell shape is defined by parametric profiles ($R(s)$, $Z(s)$), which are the radial and longitudinal components of the material point coordinates; the deformed shape is similarly defined by profiles ($r(s)$, $z(s)$); s is an arc-length measured from the mid cell. During division, deformed and undeformed shapes are changed by cell wall growth and remodeling (green regions indicate where most of the growth and remodeling occurs). Our model combines the mechanical properties of the cell wall with the growth and remodeling kinetics to compute the cell shape during division.

turgor pressure of 3–15 atm (25, 26). This implies that the wall is under constant tension, much like an inflated balloon; just like a balloon, when the internal pressure and all other tensions are removed, the cell wall will relax to an undeformed shape. To compute the response of the bacterial cell under force, we must consider the difference between the undeformed (reference) shape, and the instantaneous (deformed) shape (Fig. 1). The undeformed shape is described by mathematical functions ($R(s)$, $Z(s)$), which can be measured if internal pressure of the cell is relieved. The instantaneous shape ($r(s)$, $z(s)$) is the shape observed in the microscope. The difference between the deformed and undeformed shapes is explained by the mechanical properties of the cell wall. These factors can be quantified in an elastic energy, $E(r(s), z(s), R(s), Z(s))$, which is a function of the instantaneous shape and the undeformed shape. This energy contains bending, stretching, and actions from forces, such as those coming from the Z-ring and internal pressure. Given an undeformed shape, we can compute the instantaneous shape, using a force balance equation or minimizing the energy (see *SI Text* for details).

The cell wall also has a specific structure; PG strands are not randomly oriented. In *E. coli*, for example, it appears that PG strands are perpendicular to the longitudinal direction, which suggests that the mechanical properties of the cell wall are anisotropic. Mechanical constants in the hoop (radial) and longitudinal directions are different (12, 21, 22). Anisotropic properties of the cell wall can be modeled by introducing different bending and stretching constants in the circumferential and longitudinal directions. These constants are also related to Young's moduli in those directions that have been estimated in experiments. Some of the constants used in the model are summarized in Table 1.

Cell Wall Growth and Remodeling. Having a properly defined wall elastic energy is not sufficient to describe the division dynamics. As we have noted, cell wall growth and turnover, which occur along the cylindrical part of the cell, also must be included. There is evidence for a 3-for-1 mechanism for the incorporation of new strands in *E. coli* (7, 11, 16). Three new, parallel strands are laid down just beneath an existing strand. The end strands are cross-linked together, and the old middle strand is depolymerized. Alternative scenarios without removal of strands have been proposed (12). In our model, the removal of the old strands is not crucial. However, because new strands are added to the current deformed shape, the growth mechanism should change undeformed configuration. Therefore, the undeformed shape ($R(s)$, $Z(s)$) is dynamic and a function of time. Additional equations are needed to describe the changes in ($R(s)$, $Z(s)$). The physical picture described by these equations is summarized in Fig. 2. For a small length segment of the cell wall, its shape can change by changing the component of the segment in the R and Z directions. The Z-component will elongate over time with a speed according to a rate of relative length change, τ_2^{-1}.

In addition to elongation in the Z-direction, the undeformed radius, R, also changes over time. A new PG strand is added from below to the instantaneous (i.e., deformed) wall (Fig. 2). The newly added and cross-linked material must conform with the current radius, r, which is different from the undeformed radius because of internal pressure and other forces (such as the contraction force from the Z-ring). Thus, over time, the undeformed radius must change and approach the current radius. The time scale of this turnover dynamics is described by another relative rate constant, τ_1^{-1}. This type of phenomena is similar to morphoelasticity described in ref. 27 for plant tendrils.

It is important to note that the newly added material cannot have an undeformed radius equal to the current radius. This would imply that the cell radius will continually increase over time because the deformed radius is always larger than the undeformed radius as a result of internal pressure. Instead, R must approach a radius smaller than r, say $(r - d)$, where $d = d_0 r$, and d_0 is a parameter.

Table 1. Parameters used in the model

Parameter	Description	*E. coli*	*B. subtilis*
Y_1	Longitudinal Young's modulus, MPa	25	13
Y_2	Circumferential Young's modulus, MPa	75	39
ΔP	Internal turgor pressure, MPa	0.3	1.5
δ	Cell wall thickness, nm	6	40
d_0	New PG prestretch amount	0.2	0.2
λ_1	Septum PBP distribution width, nm	13	17
λ_2	Septum PBP distribution width, nm	13	17
J_1	Septum PBP turnover rate (typical), s^{-1}	0.04	0.01
J_2	Septum PBP growth rate (typical), s^{-1}	0.2	0.025
J_0	Background elongation rate (typical), s^{-1}	0.001	0.001
f	Z-ring force, pN	8–80	≈50–60

MPa, 10^6 Pa or 10 atm.

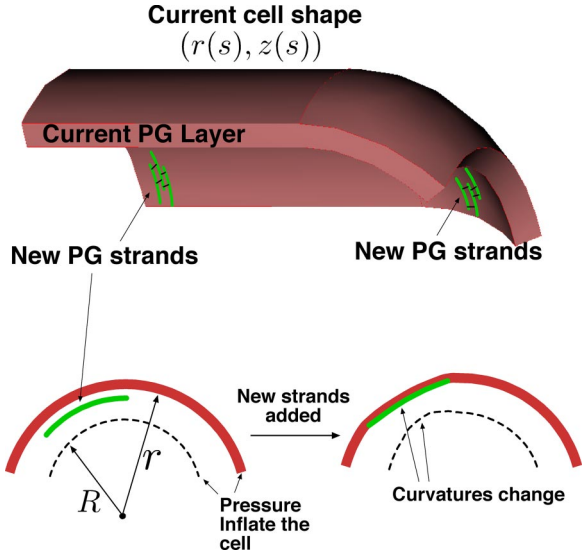

Fig. 2. Detailed view of growth and turnover of the PG cell wall, which occur by adding new PG strands and removing old ones. The newly added strands conform with the current shape ($r(s)$, $z(s)$). For example, in *Upper*, the new cell wall at *Lower Right* should conform to a smaller radius than that shown at *Lower Left*. This implies that the undeformed shape ($R(s)$, $Z(s)$) is changing. In particular, R should approach r over time (*Lower*). The cell probably adds what may be regarded as a ''prestretched'' strand during growth to maintain the wall radius. The prestretched amount is described by the parameter d_0 (see *Cell Wall Growth and Remodeling*).

This parameter models that, to act against the expanding pressure, the cell probably adds a "prestretched" PG strand or tightens the strand after it is added. The prestretched amount must be proportional to the added area; therefore, $d \propto r$. The prestretching or tightening amount is exactly d_0. d (or d_0) is determined by the Young's moduli in the radial direction and the magnitude of the turgor pressure. If the wall is stiff in the radial direction, then less tightening is needed to resist the expansion from turgor pressure. Using physiological turgor pressures in *E. coli* and *B. subtilis* and estimated Young's modulus for these species, we found by fitting that $d_0 = 0.2$ for both *E. coli* and *B. subtilis*. The same constant is sufficient for two species of bacteria, which suggests that this is a common mechanism.

In bacterial cells lacking MreB, it was found that the cell cannot maintain the rod-like shape and slowly increases in radius (28–30). Although the mechanism of MreB is not known, our model suggests that the function of MreB is related to the constant d_0. MreB possibly catalyzes the stretching step during PG addition, although our model is insufficient to give a molecular mechanism. An alternative model is to consider a possible "mechanical reenforcement" coming from the rigidity of MreB filaments. However, it should be noted that the necessary reenforcement force would be proportional to the turgor pressure, which is vastly different in *E. coli* and *B. subtilis*. It is unclear whether MreB is mechanically different in different species of bacteria.

Growth and Remodeling Kinetics. Finally, time constants associated with changes in R and Z, τ_1 and τ_2, are also functions of the arc-length along the cell in our model. Growth and turnover can occur faster near the Z-ring. PBPs have been found to localize near the mid cell during division. Elongation and turnover rates must be proportional to the local PBP concentration; therefore, we introduce exponential functions for $\tau_1(s)$ and $\tau_2(s)$, modeling the spatial variations in PBP concentration:

$$\frac{1}{\tau_1(s)} = J_1 e^{-s/\lambda_1}$$

$$\frac{1}{\tau_2(s)} = J_2 e^{-s/\lambda_2} + J_0, \qquad [1]$$

where parameters $\lambda_{1,2}$ describe the width of the PBP distribution around the mid cell, and J_0 is the elongation rate of the cylindrical region resulting from the diffusively located PBPs. Through trial and error, we found $\lambda_{1,2}$ to be ≈15 nm, suggesting that division-related remodeling is concentrated around a ±50 nm region near the Z-ring. This is consistent with available data on localization of PBPs (10). $J_{1,2}$ are the maximum rates at mid cell. The spatial dependences of $\tau_1(s)$ and $\tau_2(s)$ have a large effect on the shape of the cell during division (see *Results*).

Thus, the Z-ring has two roles in this model: One is to generate a force that slightly changes the cell radius and establish the direction where the new wall can grow. The other role is to enhance the growth and turnover speeds near the mid cell so that the wall is remodeled there. The newly grown cell wall has a furrow, and therefore Z-ring does not have to completely overcome turgor pressure to decrease the cell radius further.

Results

If there is no growth and turnover in the cell wall, the model predicts that an extraordinarily large force is necessary to achieve contraction. From the estimated Young's moduli for *E. coli* and *B. subtilis* cell walls, and the known wall thickness, the bending constants are ≈10^4 pNnm and ≈10^6 pNnm, respectively. The stretching moduli are also substantial (300–1,000 pN/nm). If the cell wall is static, then it requires ≈400 pN to deform the cell radius by 200 nm. The energetic source for such a force is unclear. More importantly, the time for achieving this deformation is determined by the viscous drag experienced by the cell wall, which gives a contraction speed of the order 0.1 s, much faster than the contraction time of minutes observed in live cells.

With a growing cell, the situation changes. Solutions to four equations discussed in *SI Text* provide estimates for the cell shape during contraction and the necessary Z-ring force and growth and turnover rates. Fig. 3 shows computed cell shapes for *E. coli* with a Z-ring force of $f = 8$ pN and $f = 80$ pN. The initial cell shape was a perfect rod. The cell has contracted from a radius of 500 nm to 250 nm. The contraction time varies, depending on the growth and turnover rates. For $J_1 \approx 0.05\ s^{-1}$ and $J_2 \approx 0.1\ s^{-1}$, the contraction finishes in 3–5 min, giving a contraction velocity of ≈ 1 nm/s. Here, the growth rate τ_1^{-1} and turnover rate $\tau_2^{-1}$are described by Eq. **2**, and $\lambda_{1,2} = 13$ nm, indicating that the PBPs are concentrated in a region of ±50 nm around the division site. Because growth and turnover are concentrated near the furrow, the length of the bacteria increases linearly with time during the division phase.

In *E. coli*, it was estimated that the cell turns over all of its wall material in approximately two life cycles (18). If the cell cycle is ≈20 min, then the turnover rate or J_2^{-1} should be around minutes.

A result of our modeling is that the division can succeed for a wide range of Z-ring force between 8 pN and 80 pN. Not surprisingly, the growth and remodeling rates are important factors in determining the cell shape; however, the Z-ring force is not a critical factor, at least for *E. coli*. Fig. 3 shows several examples of cells with different combinations of growth and remodeling behavior. We see that several combinations can produce qualitatively correct cell shapes (Fig. 3 *A* and *B*). However, an unphysical growth-rate function will produce incorrect cell shapes (Fig. 3*C*). The model also correctly predicts the shapes of minicells produced by *E. coli* mutants (Fig. 3*D*).

In Gram-positive *B. subtilis*, the wall Young's modulus is smaller. However, the wall is thicker. Therefore, the bending modulus of the *B. subtilis* cell wall is larger than that of *E. coli* by a factor of 100. Here, significant Z-ring force is necessary to produce any deformations, and the distribution of PBP must be

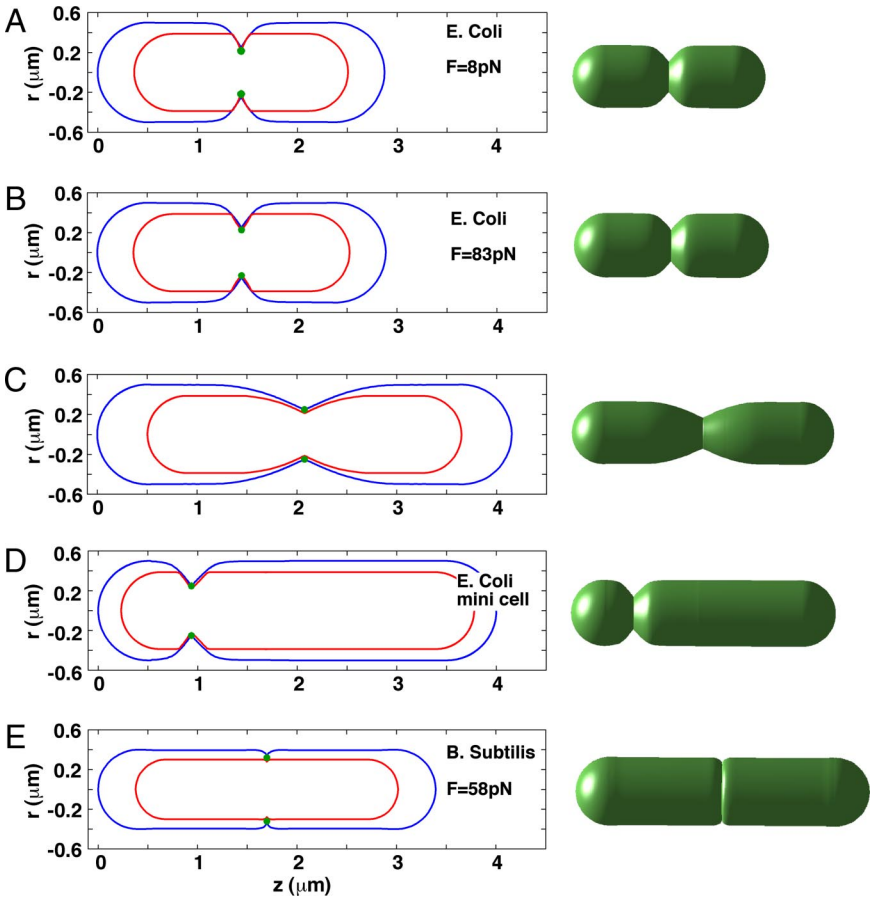

Fig. 3. Cell shapes obtained from our model with different combinations of parameters. (*Left*) The blue line is the instantaneous cell shape ($r(s)$, $z(s)$), and the red line is the undeformed cell shape ($R(s)$, $Z(s)$). (*Right*) Rendered 3D instantaneous shapes. (*A*) The shape of *E. coli* after 8 min of contraction under 8 pN of Z-ring force. Growth and turnover are confined within ±50 nm around the Z-ring. (*B*) An *E. coli* cell shape with 80 pN of Z-ring force. The cell shape appears to be relatively independent of the force. The contraction time is 2 min. (*C*) An *E. coli* cell shape with broader growth and turnover regions ($\lambda_{1,2} \approx 25$ nm). The cell shape appears unrealistic. (*D*) An *E. coli* minicell produced by contracting near the spherical cap. This phenotype occurs in mutants. (*E*) A *B. subtilis* cell shape with 58 pN of Z-ring force. Further contraction in this case is difficult because of the thick cell wall.

concentrated near the Z-ring. These factors produce the shape seen in Fig. 3*E*; any subsequent growth of the cell wall will introduce a septum structure (vertical cell wall). Fig. 3*E* is similar to electron microscopy photos of dividing *B. subtilis* where the division furrow is narrow and quite sharp (31).

Fig. 4 displays the dependence of average contraction velocity on growth and turnover rates for *E. coli*. The contraction velocity is not constant, and the average velocity is taken after contracting 250 nm. The growth rate has little effect on the contraction, but the turnover rate is important. The role of the Z-ring force is seen to speed up contraction, although only linearly. The growth and turnover rates are proportional to each other, i.e., $J_2 \propto J_1$. However, the absolute values of $J_{1,2}$ are related to the growth conditions of the cell.

The dependence of the Z-ring radius as a function of time is shown in Fig. 4 *Inset*. The radius change is gradual initially and accelerates slightly as contraction proceeds. The displayed behavior results from the relative time scales of τ_1 and τ_2. It is also possible to obtain roughly constant contraction velocities.

Depletion of MreB, an actin-like prokaryotic cytoskeletal protein, in both *E. coli* and *B. subtilis* causes the cells to grow rounder and fatter, eventually becoming spherical (28–30). This morphological transition occurs over a few division cycles. It is possible that our phenomenological parameter, d_0, is related to the function of MreB. To explore this hypothesis, we looked at the shapes of our simulated cell when the parameter d_0 was set to zero. For this case, the cell grew rounder and fatter, and the time course for the deformation was on order of the division time scale. Fig. 5 shows the shapes of a cell before and after setting $d_0 = 0$. The simulated shape when $d_0 = 0$ is strikingly similar to the shape of MreB-depleted *B. subtilis* cells after five doubling times (30). Our model also predicts that when the turgor pressure is removed, the cell shrinks up to 50% in volume and 20% longitudinally and radially. These predictions are in accord with experimental observations (21, 32).

Discussion

We have developed a dynamic model to understand the shape and mechanics of dividing rod-like bacteria. Cell shapes during division are the combined results of Z-ring force, cell wall growth, and cell wall turnover. The Z-ring force determines the direction of cell wall growth and indirectly determines the cell shape. The obtained results suggest that reasonable parameters for growth and turnover rates can reproduce physiologically observed shapes. The model also predicts realistic shapes and division times for inaccurate placement of the division site, such as those that occur for mini cells that lack the Min proteins. For other bacterial cells, such as *Caulobacter crescentus*, the basic approach should be equally valid; however, because these cells are asymmetric, a more sophisticated model for the cell wall mechanics is necessary. The basic model is also applicable to division in eukaryotic cells, such as budding and fission yeast (33) and plant cells that also have rigid cell walls. For

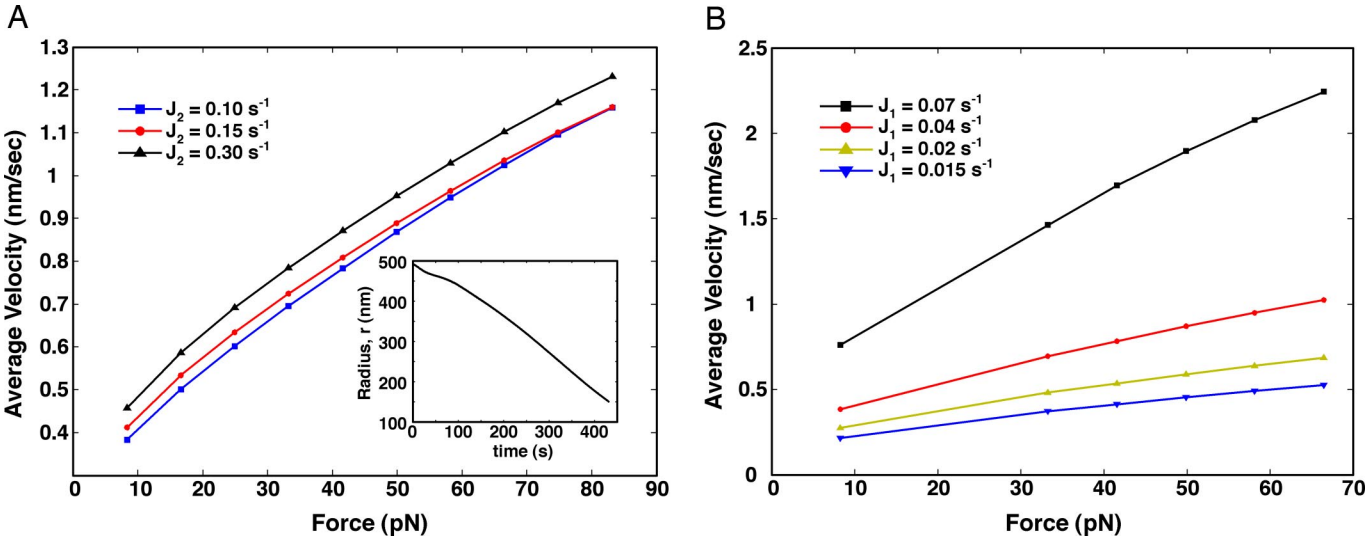

Fig. 4. Quantitative results from the model. (*A*) Average contraction velocity for *E. coli* as a function of the Z-ring force when the growth rate, τ_2^{-1} is changed. Tripling the growth rate does not affect the contraction velocity appreciably. (*Inset*) Typical division furrow radius versus time. (*B*) The turnover rate has a pronounced effect on the contraction velocity. The cell actively remodels the furrow region to achieve division.

eukaryotic cells without rigid walls, an actin cortex often maintains the shape of the cell. Whether growth and remodeling of the cortex are important will depend on the mechanical properties of the cortex and the magnitude of the contractile force from the actin-myosin contractile ring.

The molecular mechanism of FtsZ-ring contraction is currently unknown. To our knowledge, our model provides the first estimate of the force necessary to produce ring contraction and found that, with reasonable parameters, the Z-ring force is small. Indeed, in our model, we can use a constant force or a gradually decreasing force as the radius gets smaller (from 8 pN to 3 pN in the case of *E. coli*). In either case, contraction succeeds. Thus, the role of the Z-ring seems to be two-fold. One role is to generate a small force to establish the direction of cell wall growth. The other role is to concentrate the growth and enhance cell wall turnover near the ring. The result seems to generate a new undeformed shape with a furrow at the mid cell. The Z-ring does not have to act against internal pressure because the undeformed shape already has the appropriate shape. The mechanism of Z-ring force generation seems to be indirectly related to FtsZ GTPase activity (34, 35). The estimated force is small when compared with eukaryotic motors, which exert between 2 pN and 50 pN per molecule. Such forces can be derived from multiple sources and mechanisms, including collective forces from thermodynamic "phase transitions."

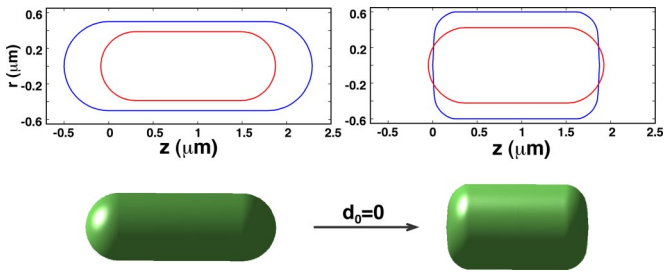

Fig. 5. The model predicts that the cell will continually increase in radius when d_0 is set to zero (see *The Model* and *SI Text*). (*Upper*) Shown are the instantaneous (blue) and the undeformed (red) shapes of the cell before (*Left*) and after (*Right*) d_0 is set to zero. (*Lower*) 3D renderings showing the change in the cell aspect ratio.

We have introduced a model to describe the growth and turnover of the bacterial cell wall. Active changes in the undeformed (reference) shape, and especially in the undeformed radius $R(s)$, are essential in producing the correct furrow shape. The basic idea can be understood qualitatively like this: Imagine a balloon that is inflated. If new unstretched material is inserted into the balloon, the balloon will expand because of two factors. First, the newly inserted material displaces the old material; and second, the new material stretches. The only way to prevent the expansion due to stretching is to insert material that is prestretched, or tightened after insertion. This mechanism is accounted for in the model by the parameter d_0, which models the prestretched amount (see *Discussion* and *SI Text*). We showed that removing this parameter causes a rod-shaped cell to expand radially, becoming more spherical (Fig. 5). The dynamics of the cell shape is similar (in both appearance and time scale) to cells that are depleted of the actin-like protein MreB.

The proposed growth and turnover model can be experimentally checked by an atomic force microscope. An atomic force microscope tip can be used to measure the force necessary to indent the cell wall and apply a constant deformation during the growing phase of the bacterium. Initially, the measured force would be large, but growth and turnover will remodel the cell wall to accommodate the new geometry. The measured force is predicted to relax over time. The measured morphoelastic time scale would be related to the growth and turnover time scale in the model.

Finally, the spatial distribution of PBP synthesis and turnover in our model is quite simple. Actual measurements show complex organization, much of which is related to MreB and Mbl. These measurements can be incorporated in a refined version of the current model without assuming cylindrical symmetry. All of the growth and turnover rates discussed in the model should also be functions of elastic stress in the cell wall.

The observed PBP localization may be explained by varying effects of the elastic stress on the PBP binding and synthesis rates. Experimentally, the force dependence of PBP synthesis rates can be tested by applying forces to different regions of the cell. The present model can be used to analyze the growth rates when cells are subjected to different forces.

We thank Alex Dakjovic and Joe Lutkenhaus for helpful discussions. This work was supported by National Institutes of Health Grant GM075305.

1. Bi EF, Lutkenhaus J (1991) *Nature* 354:161–164.
2. Dajkovic A, Lutkenhaus J (2006) *J Mol Microbiol Biotechnol* 11:140–151.
3. Lutkenhaus J (2007) *Annu Rev Biochem* 76:539–562.
4. Raskin DM, de Boer PA (1999) *Proc Natl Acad Sci USA* 96:4971–4976.
5. Rothfield L, Taghbalout A, Shih YL (2005) *Nat Rev Microbiol* 3:959–968.
6. Sun Q, Margolin W (1998) *J Bacteriol* 180:2050–2056.
7. Bramhill D (1997) *Annu Rev Cell Dev Biol* 13:395–424.
8. Pogliano J, Pogliano K, Weiss DS, Losick R, Beckwith J (1997) *Proc Natl Acad Sci USA* 94:559–564.
9. Errington J, Daniel RA, Scheffers DJ (2003) *Microbiol Mol Biol Rev* 67:52–65.
10. Scheffers DJ, Jones LJ, Errington J (2004) *Mol Microbiol* 51:749–764.
11. Höltje JV (1998) *Microbiol Mol Biol Rev* 62:181–203.
12. Cooper S (1991) *Microbiol Rev* 55:649–674.
13. Cooper S (1991) *Bacterial Growth and Division, Biochemistry and Regulation of Prokaryotic and Eukaryotic Division Cycles* (Academic, San Diego).
14. Den Blaauwen T, Aarsman ME, Vischer NO, Nanninga N (2003) *Mol Microbiol* 47:539–547.
15. Wang L, Khattar MK, Donachie WD, Lutkenhaus J (1998) *J Bacteriol* 180:2810–2816.
16. Höltje JV (1996) *Microbiol* 142:1911–1918.
17. Pooley HM (1976) *J Bacteriol* 125:1127–1138.
18. Park JT (2001) *J Bacteriol* 183:3842–3847.
19. Park JT (1993) *J Bacteriol* 175:7–11.
20. de Pedro MA, Quintela JC, Höltje JV, Schwarz H (1997) *J Bacteriol* 179:2823–2834.
21. Thwaites JJ, Mendelson NH (1991) *Adv Microb Physiol* 32:173–222.
22. Yao X, Jericho M, Pink D, Beveridge T (1999) *J Bacteriol* 181:6865–6875.
23. Thwaites JJ, Mendelson NH (1985) *Proc Natl Acad Sci USA* 82:2163–2167.
24. Matias VR, Beveridge TJ (2005) *Mol Microbiol* 56:240–251.
25. Koch AL, Lane SL, Miller JA, Nickens DG (1987) *J Bacteriol* 169:1979–1984.
26. Woldringh CL (1994) *Mol Microbiol* 14:597–607.
27. Goldstein RE, Goriely A (2006) *Phys Rev E* 74:010901.
28. Wachi M, Doi M, Tamaki S, Park W, Nakajima-Iijima S, Matsuhashi M (1987) *J Bacteriol* 169:4935–4940.
29. Doi M, Wachi M, Ishino F, Tomioka S, Ito M, Sakagami Y, Suzuki A, Matsuhashi M (1988) *J Bacteriol* 170:4619–4624.
30. Jones LJ, Carballido-Lopez R, Errington J (2001) *Cell* 104:913–922.
31. For example, Koch AL (2001) *Bacterial Growth and Form* (Kluwer Academic, Norwell, MA), p 241.
32. Koch AL, Woeste S (1992) *J Bacteriol* 174:4811–4819.
33. Wu JQ, Kuhn JR, Kovar DR, Pollard TD (2003) *Dev Cell* 5:723–734.
34. Bi EF, Lutkenhaus J (1992) *J Bacteriol* 174:5414–5423.
35. Mukherjee A, Saez C, Lutkenhaus J (2001) *J Bacteriol* 183:7190–7197.